

Investigation of Superconducting Gap Structure in $\text{TbFeAsO}_{0.9}\text{F}_{0.1}$ using Point Contact Andreev Reflection

K A Yates^{1,3}, K. Morrison¹, Jennifer A. Rodgers², George B. S. Penny², Jan-Willem G. Bos², J. Paul Attfield², and L F Cohen¹

¹The Blackett Laboratory, Physics Department, Imperial College London, SW7 2AZ, UK

²Centre for Science at Extreme Conditions and School of Chemistry, University of Edinburgh, King's Buildings, Mayfield Road, Edinburgh, EH9 3JZ.

Bulk samples of $\text{TbFeAsO}_{0.9}\text{F}_{0.1}$ ($T_c^{\text{on}} = 50\text{K}$) were measured by point contact Andreev reflection spectroscopy. The spectra show unambiguous evidence for multiple gap-like features plus the presence of high bias shoulders. By measuring the spectra as a function of temperature with both gold and superconducting niobium tips, we establish that the gap-like features are associated with superconducting order parameter in this material. We discuss whether the well defined zero bias conductance peak that we observe infrequently is associated with a nodal superconducting order parameter.

PACS: 74.25.Fy, 74.45+c

³ Corresponding author, Karen A Yates, e-mail: k.yates@imperial.ac.uk

1. Introduction

Since the discovery of superconductivity at 26K in fluorine doped $\text{LaFeAsO}_{1-x}\text{F}_x$ ¹ there has been considerable experimental and theoretical work devoted to fundamental questions related to the nature of the superconductivity in these materials. Many theoretical models suggest that the gap order is unconventional with nodes in the gap structure^{2,3}, multigap extended s-wave symmetry⁴ or some combination thereof. Experimentally, the order parameter has been interpreted as both nodeless^{5,6,7,8,9} or nodal^{10,11,12,13,14} and either single gap^{9,12,13} or multiply gapped^{8,14,15}. There is little consensus yet partly due to consistency across the samples, partly owing to the role played by rare earth substitution and the differences concerning doping with F or oxygen vacancies. At this early stage it is important that as many results as possible are shown and discussed so that some consensus can be established. In this paper, we present point contact Andreev reflection (PCAR) spectroscopy data as a function of magnetic field and temperature on high pressure synthesised samples of $\text{TbFeAsO}_{0.9}\text{F}_{0.1}$ in order to directly probe these questions. We also interrogate the sample using a superconducting niobium tip in order to examine whether the resulting sub-gap structure can validate the spectroscopic features as gap structures and whether the dimensionality of the associated Fermi surface sheets can be established.

2. Experimental Method and Data Analysis

The bulk, polycrystalline $\text{TbFeAsO}_{0.9}\text{F}_{0.1}$ samples studied here were prepared by a high pressure synthesis route as described in ref [16]. The sample was measured resistively and found to have a superconducting onset temperature of $T_c^{\text{on}} = 50\text{K}$ and a transition width $\Delta T_c \sim 3\text{K}$. Point contact Andreev reflection measurements were taken with a mechanically sharpened tip of either Au or Nb as described in detail elsewhere¹⁷. Measurements were taken at 4.2 K when both tip and sample were immersed in liquid helium and as a function of temperature and magnetic field.

We use a four point method to determine the conductance spectra by sweeping the voltage bias across the tip-sample junction and measuring the differential conductance of the ac ripple applied on top of this bias sweep. The contact size assuming one single junction contact, calculated using the Sharvin formula¹⁸ was found to be in the 3nm - 8nm range. Although this is comparable to the reported coherence length for the oxypnictides¹⁹, it is much less than the mean free path of the gold tip. Moreover, as the junction between tip and sample is made up of many tens of parallel channels²³, this means that the individual contacts are well inside the ballistic regime and consequently heating effects across the junction can be neglected.

For the analysis of the PCAR data we use the Blonder, Tinkham, Klapwijk (BTK) formalism that results in the extraction of three parameters, the superconducting energy gap Δ , the broadening parameter Γ (which incorporates thermal and non thermal broadening contributions) and the interface parameter Z which is taken to be a delta function potential at the interface²⁰. We extend this model in various ways depending on the nature of the spectroscopic data. For multiple gaps we assume that the conductance spectrum is a weighted sum of contributions from two superconducting order parameters in order to extract Δ_1 and Δ_2 ¹⁷. For data taken in magnetic field we incorporate the two channel model²¹ that allows a proper description for the influence of vortices (for a simple s wave superconductor), and for spectra that show a clear zero bias conductance peak we incorporate the model by Kashiwaya-Tanaka²² for a $d_{x^2-y^2}$ order parameter that results in an extra variable being introduced to the model, α , the angle between the quasiparticle injection trajectory and the superconducting order parameter antinode. Due to the introduction of a fourth fitting parameter and the associated possibility of degenerate fits²³, we adapted a $\chi^2(\alpha)$ fitting procedure that we have described in detail elsewhere (with respect to fitting the spin polarisation P of ferromagnetic materials in reference 23). In the adapted $\chi^2(\alpha)$ procedure used here, the value of α is varied incrementally and a three parameter fit (for Δ , Z and Γ) is performed in order to calculate χ^2 . The resulting plot of χ^2 vs α shows a minimum in $\chi^2(\alpha)$ that indicates the best fit to the data. However, it should be noted that in polycrystalline samples, α is expected to be an average value taken across several randomly oriented grains²⁴.

3. Results

Zero Bias Conductance Peak

We start by showing in figure 1(a) a typical example of spectroscopic data that shows the zbcpc feature and how it evolves with temperature. The zbcpc decreases in height with increasing temperature. Figure 1(b) shows the fit of the 4.2K spectra to the Kashiwaya-Tanaka $d_{x^2-y^2}$ model with $\Delta = 8.5\text{meV}$, $Z = 0.4$, $\alpha = 0.21\text{rad}$ and $\Gamma = 0.97\text{meV}$. To fit the higher temperature spectra to the same model, both the Z and α parameters have to be adjusted systematically, (Z by 20% and α by 10%) which is rather unphysical given the fact that the contact resistance at high bias was constant with increasing temperature, suggesting a stable contact and therefore fixed values of these parameters. We can project how we expect the spectra to evolve as a function of temperature if subjected only to increased thermal broadening using the fitted values for the 4.2K data. In order to compare directly to experiment we show the ratio of the height of the zbcpc compared to that of the finite bias conductance peak, figure 2. Clearly the experimental variation of the zbcpc is inconsistent with a simple d-wave scenario to explain the zbcpc. Samuely et al,¹¹ have already noted that the temperature dependence of the zbcpc peak is unusual within the context of a simple d-wave superconductor, although the observed temperature dependence in that paper differs significantly from that reported here. Furthermore, we observe no splitting of the zbcpc with magnetic field (figure 1c) as may be expected for a d-wave superconductor²⁵, although this may be a consequence of the orientation of the contact with respect to the superconductor crystal axis.

In order to explore the hypothesis that a Josephson junction in series with the contact is responsible for the zbcpc²⁴ we study the field evolution of a different set of spectra that also show the zbcpc anomaly. The results are shown in figure 1(c). A Josephson junction would be expected to show a rapid decrease in zbcpc height with increasing magnetic field which is not observed. The spectra are therefore inconsistent with either a d-wave order parameter or a simple, single s-wave order parameter with a Josephson junction in series with the contact. Therefore, in contrast to recent STM data¹⁰, a single gap of either s or $d_{x^2-y^2}$ symmetry cannot explain the data presented here.

Multigap Features

We now turn to examine spectra taken from a different region of the same polycrystalline sample, that do not show the zbcpc such as the example shown in figure 3. This data is unusual because it shows two clear peaks in the conductance curves at $V \approx 4.5\text{mV}$ and $V \approx 8.6\text{mV}$ suggesting the possible observation of multigap superconductivity. Note that at 4.2 K, only one broad gap feature is evident in the point contact spectrum at $\sim 5.4\text{--}6\text{meV}$, although there is a weak shoulder on the data at $V \sim 8.8\text{meV}$. As the temperature is increased to 5 K two peaks become clearly discernable in the spectra. (Note that the observation of a change in the spectra at low temperature is a common feature in this material and might be associated with magnetic ordering of Tb at low temperatures. This effect is not discussed further here). If both peaks are associated with superconducting gaps, then, for a sample where $T_c = 50\text{K}$, the BCS ratio ($2\Delta/kT_c$) is 2.1 and 3.9 respectively. In figure 4 we fit the 5K data shown in figure 3 using the 2 s-wave order parameter analysis¹⁷. This gives $\Delta_1 = 5.0\text{meV}$ and $\Delta_2 = 8.8\text{meV}$ with $Z = 0.37$, broadening parameter $\Gamma = 0.65\text{meV}$ and a weighting factor between the two gaps of $f = 0.42$. Figure 4 also shows typical example fits to other spectra where unlike curve (a) two gaps are not well resolved but the spectra peak is broad, including (c) the 4.2K spectrum in figure 1a. It is interesting to note that for similar temperatures, all spectra give similar energy gap values and similar values for the breadth of this peak feature, whether the peaks are resolved or not.

Dimensionality

Up until this point we have presented data that addresses the symmetry and multigap nature of these materials. In order to examine the dimensionality of the superconductivity we extend the experiments to include interrogation using a Nb tip as a function of temperature above and below $T_c(\text{Nb})$. The results shown in figure 5 are preliminary but interesting. The theory to describe the conductance resulting from a point contact between two superconducting materials was developed by Octavio et al²⁶ and results in the

observation of sub-gap structure which appears as peaks in the conductance of the junction²⁷. Previously this method was used for the two gap superconductor, MgB₂, to demonstrate that, although in principle sub-gap features should appear at Δ_i/n ($n=1,2,3$ etc and $i = \Delta_{\text{Nb}}, \Delta_{\sigma,\pi}$) and $(\Delta_{\text{Nb}}+\Delta_{\pi,\sigma})/m$ (where $m= 1,3,5$ etc), only the gap Δ_π associated with the three dimensional Fermi surface participated in the process²⁸.

Measuring the point contact spectrum of the TbFeAsO_{0.9}F_{0.1} with a Nb tip at $T = 11\text{K}$ (normal state of Nb) and $T < T_c(\text{Nb})$ (9.2K) ought to give some indication of features associated with the superconducting energy gaps that participate in the development of sub-gap structure. Figure 5 shows the conductance spectra of the TbFeAsO_{0.9}F_{0.1} with a Nb tip at 5.6K and 10K. Figure 5(a) shows that in addition to a prominent zbcpc associated with the Josephson current across the Nb- oxyaptnictide junction, significant enhancement in the conductance is also observed in two bias regions at $V \leq |8\text{mV}|$ and $|8\text{mV}| < V \leq |30\text{mV}|$. At low bias voltages there are clear sub-gap structure peaks which move to increasingly lower bias as the temperature is raised, as shown in figure 5(b). By tracking these peaks in the conductance as a function of temperature the first peak is associated with Δ_{Nb} (1.5meV). There are clearly several additional peaks at higher voltages (a broad feature at 2.0 ± 0.4 mV, $3.5 \pm 0.2\text{mV}$, $4.6 \pm 0.4\text{mV}$) that indicates that coupling between the two superconductors exists. By assuming gap values of $\Delta_1 = 5.0\text{meV}$ and $\Delta_2 = 8.8$ meV, we can tentatively assign these peaks to $\Delta_1/3$, $(\Delta_2+\Delta_{\text{Nb}})/5$, or $(\Delta_1+\Delta_{\text{Nb}})/3$; $(\Delta_2+\Delta_{\text{Nb}})/3$ and Δ_1 or $\Delta_2/2$ respectively. Clearly these results are promising but preliminary.

4. Discussion

Since the literature on the oxyaptnictides is extensive we summarise the position with respect to PCAR data to date. There have been attempts to explain the experimental PCAR results based on an unconventional order parameter either of the $s\pm$ type proposed originally by Mazin et al⁴, or the s_{xy} type proposed by Seo et al.^{29, 30, 31, 32}. For completion we include a summary of the PCAR and STM results on a variety of materials systems in table 1. One key observation that led some early PCAR and STM studies to conclude that the order parameter was d-wave was the presence in the conductance spectra of a zero bias conductance peak (zbcpc) or V shaped zero bias feature^{10, 12, 13, 14, 33}, although other studies showed spectra that could be fitted well with a simple, s-wave model⁹, or which had no zero bias anomaly^{8, 33}. Indeed, it is perfectly feasible that zbcpc can appear in spectra from polycrystalline superconductors without d-wave symmetry by Josephson effects occurring in series with the contact²⁴. The presence of a zbcpc is therefore not necessarily indicative of a d-wave order parameter. The need for caution in interpreting this zbcpc as d-wave has been further emphasised by the theoretical work investigating the consequences to tunnelling measurements of the $s\pm$ ($s\pi$) state. In these works it was not only shown that the zbcpc can be a natural consequence of the $s\pm$ ($s\pi$) state³⁰, (although there has recently been discussion about this point³⁴), it was also shown that the V shaped conductance can arise from increased impurity scattering³¹ or electron doping³². Even if Josephson effects can be ruled out as a cause of a zbcpc in a spectrum as we have done here, the presence of a zbcpc is consistent with both d-wave and $s\pm$ ($s\pi$) order parameters.

Table 1 Summary of PCAR and STM results on the gap structure of a variety of oxyarsenide samples. * indicates the current study.

Composition	Technique	Polycrystal/ Single crystal	T _c (K)	Number of gaps observed	v-shape or zbcpc	2 Δ/kT_c of gaps observed
(Ba _{0.55} K _{0.45})Fe ₂ As ₂	PCAR [15]	single	23-27	2	No	1.8-4.6 8.3-10.2
Sr _{1-x} K _x Fe ₂ As ₂	STM [12]	Poly	32	1	V	7.25
SmFeAsO _{0.85}	STM [10]	Poly	52	1	V shape	3.55-3.8
SmFeAsO _{0.85} F _{0.15}	PCAR [9]	poly	42	1	No	3.68
SmFeAsO _{0.9} F _{0.1}	PCAR [14]	poly	51.5	2	Zbcpc	1.7 4.5
LaFeAsO _{0.9} F _{0.1}	PCAR [13]	Poly	28	1	Zbcpc	3.35
LaFeAsO _{0.9} F _{0.1}	PCAR [8]	Poly	27	2	No	2.4-3.95

						8.4-10.3
NdFeAsO _{0.9} F _{0.1}	PCAR [11]	poly	51	1	No	1.36-3.2
NdFeAsO _{0.85}	PCAR [33]	poly	45	1	Zbcp	3.57
TbFeAsO _{0.9} F _{0.1}	PCAR *	Poly	50	2	ometimes zbc	2.1 3.9

Although the presence of a zbc does not explicitly reveal the symmetry of the order parameter(s) PCAR can nonetheless reveal important information concerning the number of gaps in the material, provided these gaps are resolvable compared to kT . Theoretically it has been predicted within the s_{\pm} ($s\pi$) model that the magnitude of the gaps on the hole Fermi surface and the electron Fermi surface are of similar size. However, the gaps on each Fermi surface are also predicted to be doping dependent such that $\Delta_e N_h \approx \Delta_h N_e$ ^{30,31,35}. It is therefore not clear whether there ought to be two measurably distinct gaps or not. Nevertheless as can be seen in table 1 several groups have attempted to fit PCAR spectra to multiple gap models. The observations we have made are consistent with those of Wang et al, who observed two features at $2\Delta/kT_c$ of ~ 1.7 and ~ 4.5 ¹⁴ in SmFeAsO_{0.9}F_{0.1}. They are also within the range of the lower gap feature observed by Daghero et al³⁶.

Although there may be differences between the hole doped 122 systems and the electron doped 1111 systems, Szabo et al.,¹⁵ and Gonnelli et al.,⁸ have observed additional features, usually as clearly resolved high bias shoulders on the spectra which result in a gap like feature at about $2\Delta/kT_c = 7.5 - 9$ in 122 and 1111 compounds, respectively. We see shoulder like features in our data that are at similar energy scales but we have not attempted to fit them as they are generally broad and poorly resolved. It is interesting to note that it is this upper shoulder that is consistent with superconducting energy gap values found by ARPES⁶ and FTIR³⁷.

In conclusion, we have summarised the observations from the literature using the PCAR method and compared these observations to our own data. There appears to be some convergence in understanding and some aspects of the data are consistent between groups using the PCAR method. Clearly much more work needs to be done in order to understand the role of doping and impurities in these materials before we will fully understand gap symmetry, gap number and gap dimensionality. Nevertheless in the present contribution we appear to have ruled out the zbc in our PCAR data on TbFeAsO_{0.9}F_{0.1} as being directly related to a Josephson junction in series with the tip junction or to a model invoking a single d-wave order parameter. Most groups now favour a multigap scenario and several groups are fitting the high bias feature and interpreting this as a superconducting energy gap. In our case we have seen clear evidence for two well resolved spectroscopic features which are usually encompassed by one broader feature. These features may result from sample inhomogeneity and/or orientational dependence due to the polycrystalline nature of the material. Preliminary results from the superconducting Nb tip spectroscopy data suggest that both gaps individually participate in the sub-gap structure, although further work on single crystals would be needed to confirm this statement.

References

- ¹ Y Kamihara, T Watanabe, M Hirano, H Hosono, "Iron-based layered superconductor $\text{La}(\text{O}_{1-x}\text{F}_x)\text{As}$ ($x=0.05-0.12$) with $T_c = 26\text{K}$ " *J Am. Chem. Soc.*, **130**, 3296 (2008)
- ² ZY Weng, "Hidden SDW order and effective low-energy theory for FeAs superconductors", arxiv: 0804.3228v2 (2008)
- ³ J. Li and Y Wang, "The minimum model for the iron-based superconductors", *Chin. Phys. Lett.*, **25**, 2232 (2008)
- ⁴ I.I. Mazin et al, "Unconventional superconductivity with a sign reversal in the order parameter of $\text{LaFeAsO}_{1-x}\text{F}_x$ " *Phys. Rev. Lett.*, **101**, 057003 (2008)
- ⁵ L. Malone, JD Fletcher, A Serafin and A Carrington, "Magnetic penetration depth of single crystal $\text{SmFeAsO}_{1-x}\text{F}_x$: a fully gapped superconducting state", arxiv: 0806.3908 (2008)
- ⁶ H. Ding et al, "Observation of Fermi-surface dependent nodeless superconducting gaps in $\text{Ba}_{0.6}\text{K}_{0.4}\text{Fe}_2\text{As}_2$ " *Europhys. Lett.*, **83**, 47001 (2008)
- ⁷ C Martin et al, "Nodeless superconducting gap in $\text{NdFeAsO}_{0.9}\text{F}_{0.1}$ single crystals from anisotropic penetration depth studies", arxiv: 0807.0876 (2008)
- ⁸ R.S. Gonnelli, D. Daghero, M. Toretello, GA Ummarino, VA Stepanov, JS Kim, RK Kremer "Coexistence of two order parameters and a pseudogap in the iron-based superconductor $\text{LaFeAsO}_{10x}\text{F}_x$ " arxiv: 0807.3149 (2008)
- ⁹ TY Chen, Z. Tesanovic, RH Liu, XH Chen, CL Chien, "A BCS like gap in the superconductor $\text{SmFeAsO}_{0.85}\text{F}_{0.15}$ " *Nature* **453**, 1224 (2008)
- ¹⁰ O Millo, I Asulin, O Yuli, I Felner, Z-A Ren, ZX Zhao, "Scanning tunnelling spectroscopy of $\text{SmFeAsO}_{0.85}$: Possible evidence for d-wave order parameter symmetry" *Phys. Rev. B*, **78**, 092505 (2008)
- ¹¹ P Samuely, P. Szabo, Z. Pribulova, ME Tillman, S Bud'ko, PC Canfield, "Possible two-gap superconductivity in $\text{NdFeAsO}_{0.9}\text{F}_{0.1}$ probed by Point contact Andreev reflection" *Supercond. Sci. Technol* **22**, 014003 (2009)
- ¹² MC Boyer, K. Chatterjee, WD Wise, GF Chen, JL Luo, NL Wang, EW Hudson, "Scanning tunnelling microscopy of the 32K superconductor $(\text{Sr}_{1-x}\text{K}_x)\text{Fe}_2\text{As}_2$ " arxiv: 0806.4400 (2008)
- ¹³ L Shan, Y Wang, X Zhu, G Mu, L Fang, HH Wen, "Point contact spectroscopy of iron-based layered superconductor $\text{LaO}_{0.9}\text{F}_{0.1-d}\text{FeAs}$ " *Europhys. Lett.*, **83**, 57004 (2008)
- ¹⁴ YL Wang, L Shan, L Fang, P Cheng, C Ren, HH Wen, "Multiple gaps in $\text{SmFeAsO}_{0.9}\text{F}_{0.1}$ revealed by point contact spectroscopy", *Supercond. Sci. Technol*, **22**, 015018 (2009)
- ¹⁵ P. Szabo, Z. Pribulova, G. Pristas, SL. Bud'ko, PC Canfield, P Samuely, "Evidence for two-gap superconductivity and SDW pseudogap in $(\text{Ba},\text{K})\text{Fe}_2\text{As}_2$ by directional point contact Andreev reflection spectroscopy" arxiv: 0809.1566v2 (2008)
- ¹⁶ J-W. G. Bos, G. B.S. Penny, J.A. Rodgers, D. A. Sokolov, A.D. Huxley and J.P Attfield, "High pressure synthesis of late rare earth $\text{RFeAs}(\text{O},\text{F})$ superconductors; $\text{R} = \text{Tb}$ and Dy ", *Chem. Comm.*, 3634, (2008)
- ¹⁷ Y. Bugoslavsky et al, "Electron diffusivities in MgB_2 from point contact spectroscopy" *Phys Rev B*, **72**, 224506 (2005)
- ¹⁸ A. M. Duif, A. G. M. Jansen, and P. Wyder, *J Phys Cond Mat* **1**, 3157 (1989).
- ¹⁹ A.S. Sefat et al, *Phys. Rev B*, **77**, 174503 (2008)
- ²⁰ GE Blonder, M Tinkham, TM Klapwijk, *Phys Rev. B*, **25**, 4515 (1982)
- ²¹ Y Miyoshi, Y Bugoslavsky, LF Cohen, *Phys. Rev. B*, **72**, 012502 (2005)
- ²² S Kashiwaya et al, *Phys. Rev. B*, **51**, 1350 (1995)
- ²³ Y. Bugoslavsky et al, *Phys Rev B*, **71**, 104523 (2005)
- ²⁴ S. Piano et al, *Phys. Rev. B*, **73**, 064514 (2006)
- ²⁵ G Deutscher, *Rev. Mod. Phys.*, **77**, 109, (2005)
- ²⁶ Octavio et al, *Phys. Rev. B*, **27**, 6739 (1983)
- ²⁷ L.J. Barnes, *Phys. Rev.* **184**, 434 (1969)
- ²⁸ F. Giubileo et al, *Phys. Rev. B*, **72**, 174518 (2005)
- ²⁹ K Seo, B Andrei Bernevig and J Hu "Pairing symmetry in a two-orbital exchange coupling model of oxypnictides" *Phys Rev Lett*, **101**, 206404 (2008)
- ³⁰ H-Y Choi and Y Bang "Tunneling spectroscopy of π pairing state as a model for the FeAs superconductors", arxiv: 0807.4604v2 (2008)

³¹ Y Bang and H-Y Choi, “Resonant impurity scattering in the $\pm s$ gap state of the Fe-based superconductors”, arxiv: 0808.0302 (2008)

³² MM Parish, J Hu and B Andrei Bernevig, “Experimental consequences of the s-wave $\cos(kx)\cos(ky)$ superconductivity in the iron-pnictides” Phys Rev B, **78**, 144514 (2008)

³³ K.A. Yates et al, Supercond. Sci. Technol. **21**, 092003 (2008)

³⁴ J Linder and A Sudbo, “Theory of Andreev reflection in junctions with iron-based High-Tc superconductors”, Phys Rev B, 79 020501(R) (2009)

³⁵ L Benfatto, M Capone, S Caprara, C Castellani and C Di Castro, “Multiple gaps and superfluid density from interband pairing in iron oxypnictides” Phys Rev B, **78**, 140502(R) (2008)

³⁶ D. Daghero et al, private communication, (2008) ; D Daghero et al, “ Evidence for two-gap nodeless superconductivity in SmFeAsO_{0.8}F_{0.2} from Point contact Andreev reflection spectroscopy”, arxiv : 0812.1141 (2008)

³⁷ A Dubroka et al, Phys. Rev. Lett., **101**, 097011 (2008)

Figure captions:

Figure 1: (a) Temperature dependence of a contact between $\text{TbFeAsO}_{0.9}\text{F}_{0.1}$ and an Au tip showing a zbc. The spectra have been normalised and offset for clarity. (b) Fit to the 4.2K data assuming a $d_{x^2-y^2}$ order parameter and $\Delta = 8.5\text{meV}$, $Z = 0.4$, $\alpha = 0.21\text{rad}$ and $\Gamma = 0.97\text{meV}$. (c) magnetic field dependence of a contact at 8K showing a zbc. The spectra have been normalised and offset for clarity.

Figure 2: The ratio of the height of the zbc conductance to the height of the peak at finite bias, as a function T (circles). Blue triangles are the result of increased thermal broadening to the 4.2K fit. The dashed line indicates the behaviour of the zbc height if α changes from 0.21 to 0.19 or Z changes from 0.40 to 0.48

Figure 3: Temperature dependence of a contact between $\text{TbFeAsO}_{0.9}\text{F}_{0.1}$ and an Au tip showing no zbc but multiple gap like features, data have been normalised and offset for clarity.

Figure 4: Fits to three contacts from different regions of the sample using a 2 s-wave model. From top, (a) 5.6K $\Delta_1 = 5.0\text{meV}$ and $\Delta_2 = 8.8\text{meV}$, $Z = 0.37$, $\Gamma = 0.65\text{ meV}$; (b) 10K $\Delta_1 = 4.6\text{meV}$ and $\Delta_2 = 8.6\text{meV}$, $Z = 0.44$, $\Gamma = 2.58\text{ meV}$; (c) 4.2K, $\Delta_1 = 6.1\text{meV}$ and $\Delta_2 = 8.0\text{meV}$, $Z = 0.49$, $\omega = 2.56\text{ meV}$. Spectra have been normalised and offset for clarity. Data points are indicated by symbols, fit is shown by the thin red line.

Figure 5: (a) Conductance curve for a $\text{TbFeAsO}_{0.9}\text{F}_{0.1}$ - Nb tip contact at 5.6K (blue up- triangle) and 10.7K (red circle). (b) Shows a magnified low bias region for the same contact at 5.0 K (navy square), 5.6K (blue up-triangle), 5.9 K (cyan down-triangle), 10.7 K (red circle). Spectra in (b) have been normalised and offset for clarity. The arrow indicates the direction of increasing temperature.

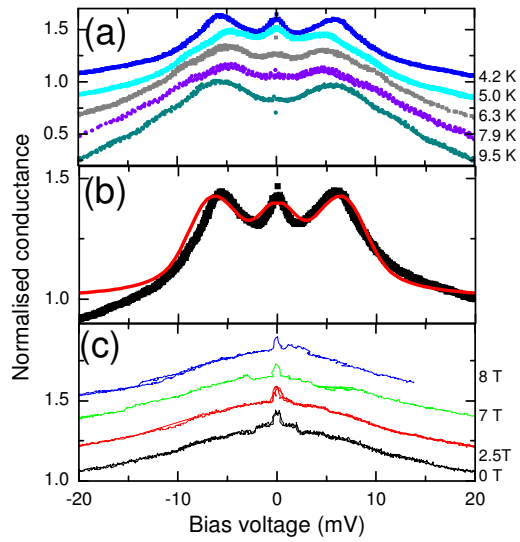


Figure 1

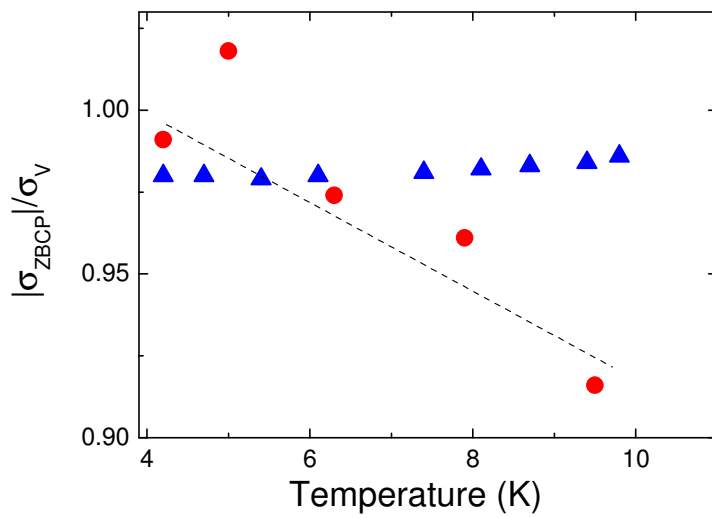


Figure 2

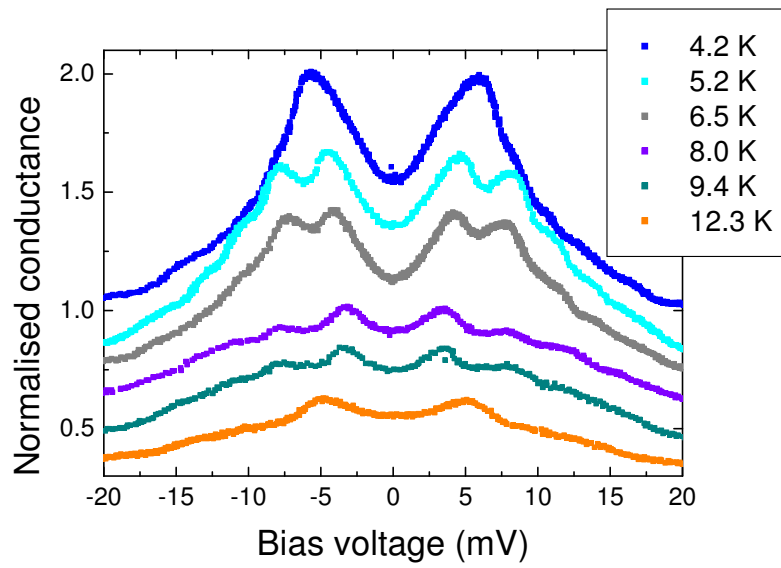


Figure 3

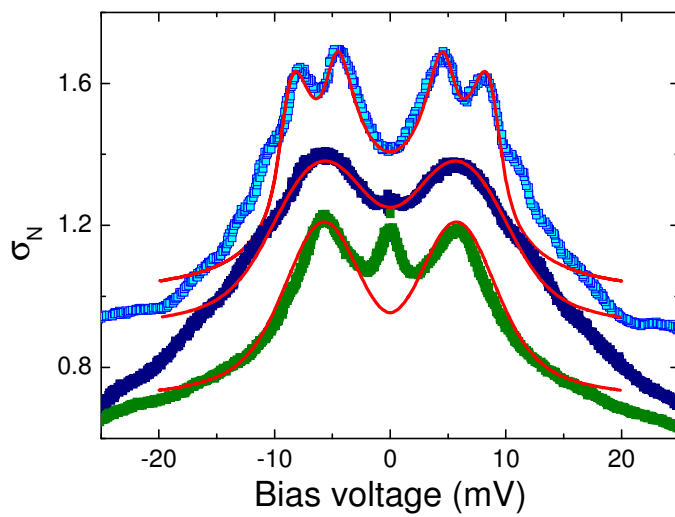


Figure 4

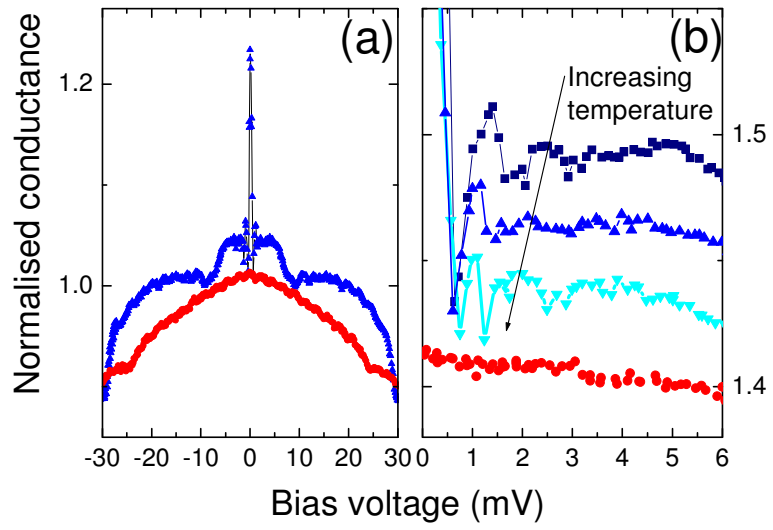


Figure 5